RSC Advances

ROYAL SOCIETY OF CHEMISTRY

www.rsc.org/advances

Poly(lactic acid) melt-spun fibers reinforced with functionalized cellulose nanocrystals

Received 00th January 20xx,
Accepted 00th January 20xx

DOI: 10.1039/x0xx00000x

www.rsc.org/

A. Mujica-Garcia,[a,b] S. Hooshmand,[c] M. Skrifvars,[d] J. M. Kenny,[a,b] K. Oksman[c] and L. Peponi [b*]

Poly(lactic acid)-cellulose nanocrystals (PLA/CNC) nanocomposite fibers with 1% weight fraction of nanocrystals were prepared by melt-spinning. In order to improve the compatibility between the PLA and the CNC, PLLA chains were grafted onto the CNC surface using a "grafting from" reaction. For comparison, melt-spun PLA fibers and nanocomposites with unmodified CNC were also prepared. The morphology, thermal and mechanical properties of the fibers with different draw ratios were evaluated. The results of this research show that the surface modification together with drawing resulted in improved fiber properties, which is expected to depend on the alignment of the CNC and of the PLA molecular chains. The modification is also expected to lead to a flexible interface which also leads to more stretchable fibers. The main conclusion is that PLLA grafting is a very promising way to improve the dispersion of CNC in PLA, creating an interfacial adhesion between the phases and making possible to spun fibers which can be drawn with improved mechanical performance.

Introduction

Nowadays, the use of high performance materials is required in many application fields, from aerospace to biomedical sector and the demand of new multifunctional materials is a key factor in both research centres than industry.[1] Moreover due to the strong increment in the consumption of polymeric-based materials, the use of biodegradable polymers is required in order to obtain environmental-friendly materials to be used in daily life products. At the same time, the attention is focused on the manufacturing and on the processing conditions of the biodegradable polymers. For example, scaffolds created from biodegradable polymers are fabricated using particulate leaching, textile technologies, or three-dimensional (3D) printing techniques.[2] At this regard, the use of polymeric fibers to form a biodegradable scaffold provides several advantages for tissue-engineering applications, because of their large surface area-to-volume ratio. Moreover, they present a high potential to provide ideal living conditions for cells due to the ability of fibers to be processed into a variety of shapes and sizes, thus achieving the required mechanical and biological properties.[3, 4, 7]
Currently, poly(lactic acid) (PLA), an aliphatic polyester, represents the most representative biodegradable and biobased polymer on the market due to its cost-competitiveness with respect to conventional not biodegradable polymers.[5, 6] In particular, PLA is a thermoplastic biodegradable polyester of great interest from the environmental point of view due to its thermoplastic processability, good biocompatibility, its biodegradability and also its good mechanical properties.[7-9] Some limitations of PLA are its poor toughness, its slow degradation rate,[10] and its low thermal stability, limiting its processing temperature.[6, 10, 11]

In order to improve the PLA properties, the preparation of nanocomposite material by adding nanoparticles to the PLA matrix is a possibility largely developed over the past years.[12-14] Among nanoparticles, the attraction for cellulose nanocrystals (CNC) to be used as nanoreinforcements in PLA matrix has recently largely increased.[15-20]
CNC are rod-like nanoparticles obtained by acid hydrolysis of cellulose fibers with diameter in the range of 3 - 20 nm and length in the range of 100 - 600 nm, depending on the cellulose source.[5] As derived from cellulose, CNC offer many advantages such as high reactivity, renewability, biodegradability, and natural abundance.[1] In addition, CNC can be used as nanoreinforcement in composite materials based on biopolymers, like PLA, due to its suitable qualities as a consequence of combination of nanoscale dimensions and high aspect ratio together with their good mechanical properties. In this way, fully biobased nanocomposites can be obtained.[15] However, polymer/cellulose nanocomposites have a drawback relative to the poor dispersion of cellulose in non-polar mediums because of their polar surface,[19] so there is an interfacial incompatibility between the hydrophobic PLA matrix and the hydrophilic CNC, occurring aggregations of CNC.[5, 21] As a consequence of the above-mentioned issues, the preparation of CNC-based nanocomposites by extrusion can be considered as an alternative to improve their compatibility. Oksman et al.[19] studied the feasibility in using extrusion to process nanocellulose-based PLA nanocomposites. They prepared a suspension of CNC, which was pumped into the polymer melt during the extrusion process. CNC were obtained previously from commercially microcrystalline cellulose (MCC). MCC were treated with N,N-dimethylacetamide (DMAc) containing lithium chloride (LiCl) to swell and partially separate the CNC. The dispersion of CNC within the PLA matrix was appreciable. The mechanical properties of nanocomposites were improved compared to reference material. However, DMAc/LiCl caused the composites degradation when processed at high-temperature.
Another way to improve their dispersion is produced when polymer chains are grafted on the surface of CNC by a covalent linkage between CNC and the grafted polymer chains.[22] So, the grafted polymer chains act as compatibilizer between the CNC and the

[a] Dipartimento di Ingegneria Civile e Ambientale, Università di Perugia, Italy.
[b] Instituto de Ciencia y Tecnología de Polímeros, ICTP-CSIC, Spain.
[c] Division of Materials Science, Composite Centre Sweden, Luleå University of Technology, Luleå, Sweden.
[d] School of Engineering, University of Borås, Borås, Sweden.
† Footnotes relating to the title and/or authors should appear here.
Electronic Supplementary Information (ESI) available: [details of any supplementary information available should be included here]. See DOI: 10.1039/x0xx00000x

polymeric matrix, improving the interfacial adhesion and as a result, optimizing the compatibility between the polymer and the CNC.[1] The improvement of the compatibility between PLA and CNC grafted with poly(L-lactic acid) (PLLA) was studied by Navarro-Baena et al. [23] They prepared films of poly(ester-urethane) based on PCL–PLLA triblock-copolymer with functionalized and unfunctionalized CNC reporting an increment in their mechanical and shape memory properties when grafted CNC were used.

Some techniques can be used in order to obtain PLA nanocomposites fibers, such as melt spinning[8, 24-26] solution spinning[27, 28] and electrospinning.[6, 29-31] From an environmental point of view, melt spinning is a technique suitable to prepared polymeric fibers. It is a solvent-free process that provides a more environmental-friendly processing method in which there is no need for solvent removal and it can be achieved high throughput and high take-up speeds. As a consequence, melt-spinning process can be considered as the main convenient commercial method to produce large quantities of fibers in the industry.[4] Moreover, the processing conditions strongly influence the final properties of the fibers as, for example, the tendency to crystallize of PLA melt-spun fibers. In fact, crystallization can be induced in the fiber axis by drawing the fiber during its formation[4] thus considering that the drawing of the fiber can orient the polymer chains in the direction of the fiber axis. Consequently, wide range of mechanical properties can be achieved for the fibers by adjusting the melt draw ratio MDR.[4] However, PLA shows tendency to undergo thermal degradation in the molten state, due to scission of polymer chains, producing melt-spun fibers with poor mechanical properties. Its degradation is dependent on time, temperature, low-molecular weight impurities and catalyst concentration.[8, 32]

In recent years, morphologies, thermal and mechanical properties of melt-spun PLA fibers have been studied. [7, 33, 34] Persson et al.[4] prepared PLA fiber-based scaffold architectures by using melt-spinning technique and solid-state drawing. The influence of process variables, as draw ratios and temperatures, on the properties of the fibers was studied preparing monofilament and multifilament fibers. They reported that the physical properties, such as crystallinity, mechanical strength and ductility can be largely controlled by drawing process, taking into account solid-state drawing and drawing temperatures.

Only few studies regarding melt-spun PLA/CNC nanocomposite fibers have been found in the literatures. John et al. [35] prepared melt spun PLA/CNC nanocomposite fibers by melt-compounding of PLA and CNC using a twin-screw extruder in which compounded pellets were generated for feeding in melt spinning. They reported that PLA/CNC fibers showed an increment of surface roughness and aggregations of CNC. Also, the fiber stiffness was not changed by the addition of the CNC probably due to the aggregation of CNC and the poor interphase between matrix and CNC. In another study reported by Blaker et al., [36] melt-spun fibers of PLA/CNC nanocomposite were prepared, comparing neat and esterified bacterial cellulose. They showed that higher fiber diameters were produced when added CNC as a consequence of the increment in the viscosity of the polymer melt and in the reduction of the draw-ratio of the fibers. In addition, they reported that the presence of CNC also enhanced the nucleation and growth of crystals and so an improvement on the mechanical properties.

In this study, melt-spun fibers of PLA and its nanocomposites were successfully prepared in two steps. Firstly, PLA nanocomposites reinforced with neat and functionalized CNC were prepared and then the fibers were obtained by melt-spinning process. The effect of the addition of CNC, both neat and grafted with PLLA on the properties of the PLA melt-spun fibers was carrying out, focusing the attention on the fiber drawing effect on the final properties of the melt-spun fibers. In order to characterize the CNC grafted with PLLA, vibrational spectroscopy techniques, such as Fourier transform infrared and Raman spectroscopy, were used, as well as thermogravimetric analysis to determine the amount of CNC and PLA in the melt-spun fibers. Molau test was used to study the interfacial interaction between the PLA matrix and functionalized CNC. Moreover, the dispersion of the nanocrystals was controlled by birefringence. The influence of temperature reached in the compounder into possible degradation process of PLA matrix was carried out by gel permeation chromatography (GPC). The influences of the drawing and the incorporation of CNC (grafted and neat) on the final structure and properties of the melt-spun fibers were examined by scanning electron microscope, thermogravimetric analysis, wide-angle X-ray diffraction, differential scanning calorimetry and tensile test.

Experimental

Materials

Poly (lactic acid) (PLA 3051D) was supply by NatureWorks (EE.UU.) with 3% of D-lactic acid monomer and a molecular weight (Mn) of 110.000 g/mol.

Cellulose nanocrystals (CNC) were synthesized by acid hydrolysis of commercial cellulose microcrystals. Microcrystalline cellulose (MCC) powder was purchased from Sigma Aldrich. Moreover, in order to increase the compatibility between the hydrophobic polymer and the hydrophilic nanocrystals, surface modifications of CNC were carrying out by “grafting from” reaction, grafting PLLA chains onto the CNC external surface obtaining CNC-g-PLLA.

L-Lactide, stannous octoate ($Sn(Oct)_2$), chloroform ($CHCl_3$), toluene, dichloromethane and N,N-dimetilformamida (DMF) were purchased from Sigma Aldrich (Spain). 1,4-dioxane was supply by VWR International.

We refer to fibers obtained by commercial polymer as PLA fibers and to the polymeric chains grafted onto the CNC surface as PLLA, because of obtained for ring opening polymerization (ROP) of L-lactide.

Synthesis of cellulose nanocrystals

CNC were prepared following the method reported in previous works by acid hydrolysis of commercial cellulose microcrystals. [37,38] Firstly, 20 g of MCC and 175 ml of sulphuric acid solution (64% (wt/wt)) were mixed in a 250 ml three-neck round-bottom flask and homogenised with a mechanical stirrer, to carrying out the hydrolysis at 45°C during 30 min in the flask. The obtained product was diluted in 4 l of deionised water in order to stop the hydrolysis reaction. Next, to remove the excess of acid, the suspension was centrifuged, obtaining 1 l of CNC suspension, which was dialysed for

5 days to neutralize the it. To purify the suspension, an ion exchange (Dowex Marathon MR-3 hydrogen and hydroxide form) was added stirring during 24 hours and removed by filtering. The pH of the CNC suspension was adjusted around 9.0 using a 1.0 % NaOH buffer solution. [38] Finally, the CNC suspension was sonicated to get a stable suspension of the nanocrystals and it was stored in fridge at 3°C to avoid bacterial growth.

CNC functionalization with PLLA chains

A surface modification of the CNC was carried out by a "grafting from" reaction, grafting PLLA chains onto the CNC surface by ROP of L-LA, using the superficial hydroxyl groups of the CNC as initiator. The modification of the cellulose was performed following a previous work reported by Navarro-Baena et al.[23] The aqueous suspension of CNC was solvent-exchanged with acetone, with dichloromethane and with dried toluene by centrifugation and re-dispersion cycles. The modification reaction took place in a three-neck round-bottom flask equipped with a condenser with a calcium chloride tube and keeping the system under nitrogen atmosphere. The monomer was dissolved in dry toluene for 10 min at 50°C. After that, the CNC dispersed in toluene was added.

The solution was heated until 80°C and 0.2 g of $Sn(Oct)_2$ was added to the mixture using a syringe as catalyst. After 24 hours, the product was dissolved in toluene to recover it. After that, centrifugation-redispersion cycles using methanol, ethanol and acetone were carried out to remove the un-reacted monomer and the no-grafted polymer. Finally, the PLLA functionalized CNC, named CNC-g-PLLA, was dissolved in $CHCl_3$ to store them.

Nanocomposites preparation

CNC and CNC-g-PLLA nanocomposites based on PLA matrix were prepared following a similar procedure described by Persson et al.[3] Firstly, PLA was dissolved in 1,4-dioxane to form a 10 wt% solution using magnetic stirring for 24 h at room temperature. At the same time, CNC and CNC-g-PLLA were dispersed separately (1 wt%) in DMF using magnetic stirring for 2 h and ultrasonication for 2 min. In the second step, to achieve homogeneous dispersion of the CNC in the dissolved PLA matrix, both the polymer solution and the CNC suspensions were mixed, stirred (2 h) and sonicated (2 min) to form nanocomposites with 1% weight fraction CNC in the final composition. Finally, PLA/CNC and PLA/CNC-g-PLLA nanocomposite microspheres were prepared using the solvent evaporation method based on the thermally induced phase separation (TIPS). [36] In particular, microspheres were formed by drop-by-drop addition of the mixtures in liquid nitrogen, to avoid agglomeration of nanoparticles by rapid quenching, followed by solvent removal using freeze-drying at -50°C for 24 h. The same process was performed to prepare neat PLA microspheres as a reference material and the three different samples were prepared (PLA, PLA/CNC and PLA/CNC-g-PLLA).

Melt-spinning and melt drawing

Nanocomposite fibers were prepared by melt-spinning of neat PLA microspheres as well as its PLA/CNC and PLA/CNC-g-PLLA in batch mode, using a 15 ml twin-screw micro-compounder, DSM Xplore (Geleen, The Netherlands) equipped with a 0.5 mm single hole spinneret.

The experiment was carried out in speed control mode with a rotation speed varied between 50 to 80 rpm with a 5 min residence time at 190°C in an argon atmosphere.

The fibers were cooled using a gentle air flow and collected with different rates on a rotating take-up roll and subsequently the melt draw ratio (MDR) was calculated based on the following equation 1:

$$MDR = (D_0/D)^2 \qquad (1)$$

where the D_0 is the spinneret diameter and D is the fiber diameter. Figure 1 shows schematic diagram of the process. Samples with varied MDR were prepared and the compositions as well as the processing parameters are summarized in Table 1. The name of samples are defined as MDR1-A and MDR1 (lower collected speeds), MDR2-A and MDR2 (higher collected speeds), and AS, as-spun. The fiber drawing was made only in the melt state. As a consequence of the elevated number of samples to analyse and in order to simplify the analysis of the results, we compare only the properties of the AS, MDR1 and MDR2 melt-spun fibers.

Table 1. Codes, compositions, diameter and melt draw ratio (MDR) of the produced fibers for the different materials obtained.

Samples codes	PLA (wt%)	CNC (wt%)	CNC-g-PLLA (wt%)	Take-up velocity* (cm/min)	Diameter*** (µm)	MDR
PLA_{AS}	100	0	0	30-100**	358 ± 4	2
PLA_{MDR1-A}	100	0	0	1125	120 ± 6	17
PLA_{MDR1}	100	0	0	2025	80 ± 1	39
PLA_{MDR2-A}	100	0	0	3150	63 ± 3	63
PLA_{MDR2}	100	0	0	4500	53 ± 3	89
PLA/CNC_{AS}	99	1	0	30-100**	491 ± 7	1
PLA/CNC_{MDR1-A}	99	1	0	1125	181 ± 14	8
PLA/CNC_{MDR1}	99	1	0	2025	79 ± 14	40
PLA/CNC_{MDR2-A}	99	1	0	3150	60 ± 13	69
PLA/CNC_{MDR2}	99	1	0	4500	47 ± 5	113
$PLA/CNC\text{-}g\text{-}PLLA_{AS}$	99	0	1	30-100**	471 ± 80	1
$PLA/CNC\text{-}g\text{-}PLLA_{MDR1-A}$	99	0	1	1125	268 ± 23	3
$PLA/CNC\text{-}g\text{-}PLLA_{MDR1}$	99	0	1	2025	122 ± 17	17
$PLA/CNC\text{-}g\text{-}PLLA_{MDR2-A}$	99	0	1	3150	86 ± 4	34
$PLA/CNC\text{-}g\text{-}PLLA_{MDR2}$	99	0	1	4500	55 ± 6	83

* Take-up velocity was calculated based on the bobbin's circumference and number of rotating per minute.

** In case of as-spun fibers, the take-up velocity was varied to avoid stretching of the fibers.

*** Diameter of the fibers was measured by a micrometer.

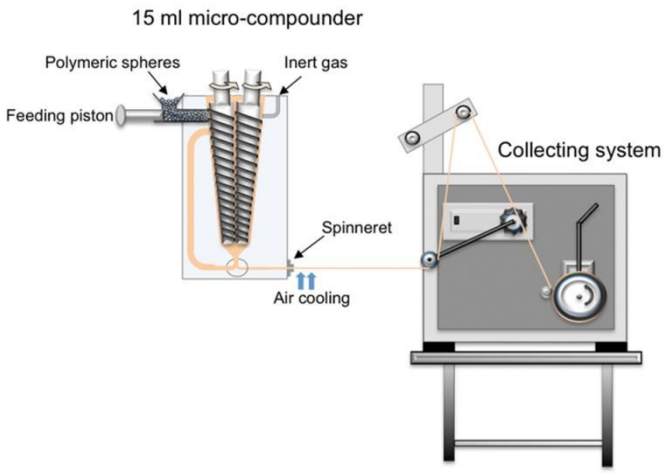

Fig. 1. Schematic diagram of melt-spinning: the compounder and the collecting roll.

Characterization

Several techniques have been used to characterize the melt-spun fibers based on PLA and PLA reinforced with neat and functionalized CNC. First, the neat CNC and the functionalized CNC-g-PLLA were characterized by vibrational spectroscopy techniques in order to verify their functionalization. Fourier transform infrared spectroscopy (FTIR) was performed on a Spectrum One FTIR spectrometer Perkin Elmer equipped with an internal reflection element of diamond in the range of 650–4,000 cm^{-1} with 1 cm^{-1} of resolution and an accumulation of 16 scans. FTIR spectra were obtained in the attenuated total reflectance (ATR) mode. Raman spectroscopy was performed by a Renishaw InVia Reflex Raman system. The Raman scattering was excited using a diode laser at a wavelength of 785 nm. The laser beam was focused on the sample with a 100 x 0.85 microscope objective. The laser power at the sample was 320 mW. The exposure was 10s and 2 accumulations for the Raman measurements. An optical microscope was coupled to the system. Also, thermogravimetric analysis (TGA) was used to determine the amount of PLLA chains grafted on the CNC surface. TGA was performed using about 10 mg of sample from room temperature to 700 °C at 10 °C/min under nitrogen atmosphere with a flow of 60 ml/min. The equipment used was a TA-TGA Q500 analyser. Moreover, TGA was used to determine also the thermal stability of the fibers.

The Molau test was used to study the interfacial interaction between the PLA matrix and CNC. [23] Three different solutions were prepared: a mixture of CNC and PLA, only CNC and CNC-g-PLLA in DMF with the concentrations used to prepare the nanocomposites. The solutions were stirred for two hours using a magnetic stirrer and them, these were laid for 48 hours at room temperature, and then, the suspensions state was carefully observed.

The flow birefringence of CNC and CNC-g-PLLA dispersions in DMF, as well as in PLA solution were studied using two polarizing filters and a lamp. The presence of flow birefringence has been considered by several authors as an indication of well dispersed CNC in organic solvents and polymer solutions. [39-42]

Morphology of melt-spun fibers was examined using a scanning electron microscopy (SEM), PHILIPS XL30 (USA). A thin layer of gold/palladium was sputter coated on the samples to minimize the charging, employing Polaron SC7640 (UK). Also, the fibers were immersed in liquid nitrogen and then fractured in order to analyse their cross-sections by SEM.

The molecular weight of the samples, before and after the melt-spinning process, was investigated by means of Gel Permeation Chromatography (GPC) using a refractomer index detector Waters 2414. 5 mg of sample were dissolved in 1 ml of filtered tetrahydrofuran (THF) and then, was filtered off using a PTFE filter before measurements. For the determination of their molecular weight, the samples were referenced to polystyrene standards between 4.000 and 400.000 g/mol.

Wide-Angle X-ray Diffraction (WAXD) measurements were achieved using a Bruker D8 Advance instrument with a Cu Kα source (0.154 nm) and a detector Vantec1. The scanning range was 2º-50º, step-size and count time per step were 0.023851º and 0.5 seconds, respectively.

Then, the thermal analysis was performed by using a differential scanning calorimetry ((DSC), Mettler Toledo DSC822e (Switzerland)) under nitrogen atmosphere. The specimens containing approximately 10 mg were mechanically sealed in aluminium pans. Thermal cycles composed by two heating scans (25 - 200 °C and -90 - 200 °C) with a cooling scan (200 - -90 ºC) in between were performed with a heating rate of 10 °C/min.

The melting temperature (T_m) and the cold crystallization temperature (T_{cc}) were taken as the maximum and minimum of the endothermic and exothermic peak from the first heating scan, respectively. Glass transition temperatures (T_g) have been calculated. The degree of crystallinity (X_c) was calculated from the melting enthalpy (ΔH_m) measured from the thermogram peak, and considering an ideal melting enthalpy for PLA ($\Delta H_{m,100}$) of 93 J/g [9], according to the following equation 2:

$$X_c = \frac{\Delta H_m}{\Delta H_{m,100\%}} \cdot 100 \qquad (2)$$

Finally, the mechanical properties of the melt-spun fibers were measured using an Instron 4411 universal test machine (Instron Corporation, Canton, MA) with single bollard grips suitable for fibers equipped with a 5 N load cell. A crosshead speed of 2 mm/min^{-1} was used and an initial grip separation of 10 mm. The samples were mounted on paper frames before being tested. Prior to testing, the fibers were conditioned in a desiccator at 23 ºC and 46% relative humidity at least for 48 h prior to the testing. The cross-section of the filaments was assumed to be circular and the diameter for each test sample was measured by a micrometer. An average value and standard deviation of 6 individual tensile determinations were reported.

Results and discussion

Several steps have been performed in order to obtain melt-spun nanocomposite fibers based on PLA and reinforced with both neat and functionalized CNC. Firstly the CNC have been synthetized and functionalized. Then, homogeneous dispersions of PLA with modified and unmodified CNC were obtained and finally, melt-spun fibers based on PLA were prepared.

Characterization of CNC functionalization with PLLA chains

In order to ensure the presence of the PLLA chain in the cellulose nanocrystals surface, vibrational spectroscopies have been used. Figure 2A shows the FTIR spectrum of PLA, CNC and CNC-g-PLLA.
The main difference between the spectra for neat and grafted CNC was the presence of the peak at 1753 cm^{-1}, corresponding to the stretching frequency of the carbonyl group in PLA and/or lactic acid oligomers. [43] Besides, the FTIR spectrums of the CNC and the CNC-g-PLLA show with the characteristic broad band in the region of 3000 cm^{-1} to 3600 cm^{-1}, corresponding of hydroxyl group present in the original cellulose structure. Also Raman spectrum (Fig. 2B) for the CNC-g-PLLA shows the characteristic bands of PLA and CNC. These results confirm the success of the grafting procedure.

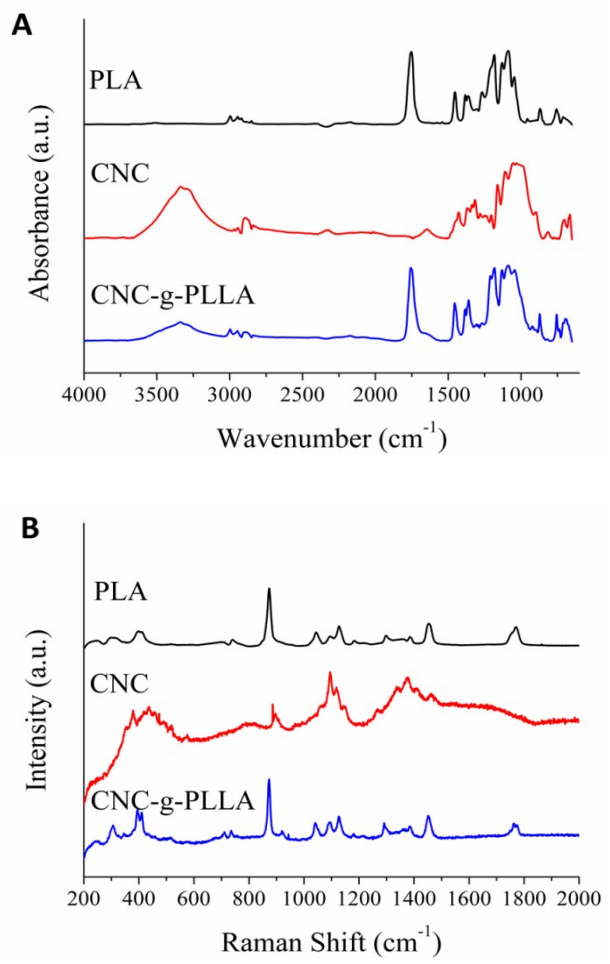

Fig. 2. Vibrational spectroscopy of CNC-g-PLLA: A) FTIR spectra and B) Raman spectra.

To determine the amount of CNC and PLLA in the CNC-g-PLLA, TGA was carried out. The weight loss and the derivative of weight loss are showed in the Figure 3. Three overlapped peaks are observed, which two of them corresponding to the thermal degradation of CNC and another to the thermal degradation of PLLA chains. In particular, CNC peaks present a maximum corresponding to 275 °C while PLLA shows the maximum peak at 230 °C.
CNC present a more broad degradation, as a consequence of different decomposition mechanism due to direct solid-to-gas phase transitions catalysed by sulphate groups on the surface, as reported in the literature. [38] The amount of the components were computed by fitting the curves with two Gaussian curves, resulting the amount of PLLA grafted chains on 67 wt% and the amount of CNC on 33 wt%. CNC peaks present a maximum corresponding to 275 °C while PLLA shows the maximum peak at 230 °C.
As it is well known, the cellulose is hydrophilic, so the dispersion of cellulose in organic solvents is poor. [23] In the Molau test, three different solutions were prepared. One of them was a mixture of CNC and PLA dissolved in DMF (vial 1), the second one was CNC dissolved in DMF (vial 2) and finally CNC-g-PLLA was dissolved DMF (vial 3), with the concentrations used to prepare the nanocomposites. Figure 4A shows the photos of the solutions taken just after stopping the stirrer process. In Figure 4B, the photos were taken laid for 48 hours. It can be observed that CNC of both neat CNC and mixture of CNC and PLA solutions precipitated. However, the suspension of functionalized CNC in the CNC-g-PLLA solution is maintained stable, as a consequence of the well-done functionalization.

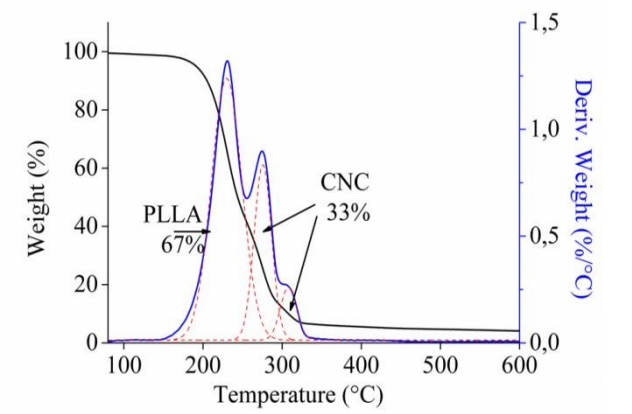

Fig. 3. Thermogravimetric analysis of functionalized CNC.

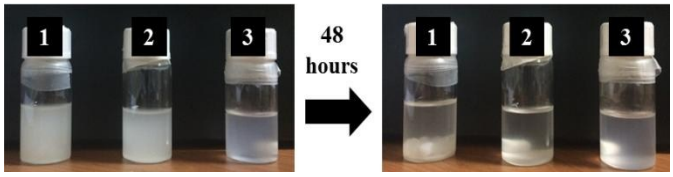

Fig. 4. Molau test results of a mixture of CNC and PLA (vial 1), of CNC (vial 2) and of CNC-g-PLLA (vial 3) in DMF.

Cellulose nanocrystals suspension characterization

To prepare nanocomposites melt-spun fibers, it is important to obtain well-dispersed nanoparticles in the polymeric matrix, because of small aggregation of the nano-reinforcements can cause spin failure. On the other hand, the surface modification of CNC is carried out to increase the compatibility between CNC and hydrophobic polymers achieving a good dispersion in non-polar solvents, making the dispersion into the biopolymers, such as PLA, easier. For these reason, a study on dispersion of neat and grafted CNC in different suspensions of DMF and 1,4-dioxane was made before the melt-spinning process of nanocomposite fibers. A study of birefringence gives an indication of the degree of association or isolation of CNC in a suspension. Therefore, the dispersion of nanoparticles in DMF, as well as in dissolved PLA, was studied using birefringence. Figure 5A and 5B show suspensions of CNC and CNC-g-PLLA in DMF respectively. Figure 5C shows the dissolved PLA in 1,4-dioxane, and Figure 5D and 5E show the suspension of CNC and CNC-g-PLLA in DMF mixed with the dissolved PLA in 1,4-dioxane. Both suspensions of CNC and CNC-g-PLLA showed the birefringence, which indicated a good dispersion of CNC in DMF without agglomeration. At the same way, the suspensions of CNC and CNC-g-PLLA mixed with the PLA solution shows the clear flow birefringence, which was not observed in the case of PLA solution indicating that the dispersion is good.

Melt-spun fibers of PLA and its PLA/CNC nanocomposite

Fiber morphology

Neat PLA and its nanocomposite fibers were successfully prepared at different melt draw ratios. Melt spinning of nanocomposite renders many challenges, mostly because fibers with their small cross section area are very sensitive for aggregated CNC, impurities and defects, which will affect the properties and can easily cause fiber breakage. Thus, having well-dispersed nanocrystals (CNC) in the PLA matrix will be a key point in the process. Otherwise the aggregated particle can cause fiber defects inducing low drawability, low strain which will lead to lower maximum strength and toughness in the fibers. As expected, the diameters of the melt-spun fibers decrease when a higher collected speed is used (Table 1). In case of PLA fibers, the diameter was reduced by ≈77 and 85% for MDR1 and MDR2, respectively compared to the as-spun one. While, the reduction in diameter caused by drawing is 84 and 90% for PLA/CNC and 77 and 88% for PLA/CNC-g-PLLA fibers when the two different MDR have been taken into account.

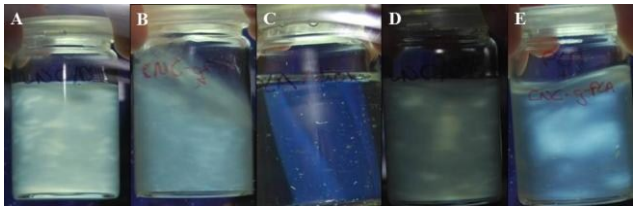

Fig. 5. Observation through crossed polarizing filters of A) CNC in DMF, B) CNC-g-PLLA in DMF, C) PLA in 1,4-dioxane, E) PLA/CNC and F) PLA/CNC-g-PLLA, showing flow birefringence of dispersions where CNC are present.

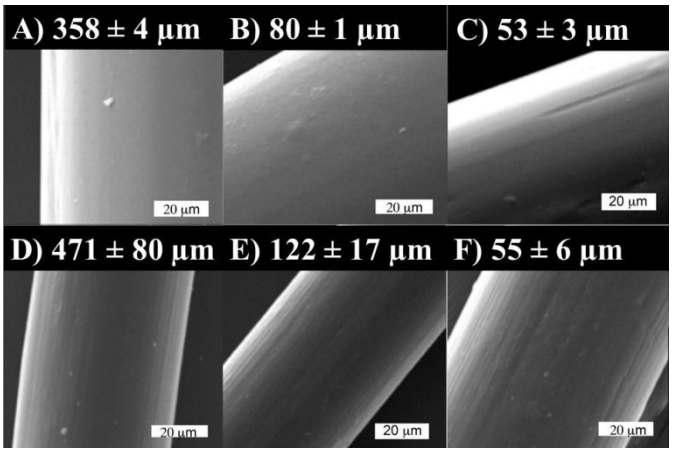

Fig. 6. SEM images of melt-spun fibers with same magnification showing surface morphology and diameter decrease from as spun to drawn fibers. A) PLA_{AS}, B) PLA/CNC_{AS}, C) $PLA/CNC\text{-}g\text{-}PLLA_{AS}$, D) PLA_{MDR2}, E) PLA/CNC_{MDR2} and F) $PLA/CNC\text{-}g\text{-}PLLA_{MDR2}$.

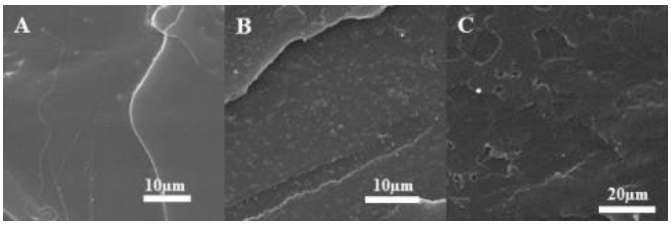

Fig. 7. SEM images of cryo-fractures surfaces of the melt-spun fibers of: A) PLA_{AS}, B) PLA/CNC_{AS} and C) $PLA/CNC\text{-}g\text{-}PLLA_{AS}$.

The surface morphology of melt spun fibers was studied by SEM and the PLA, PLA/CNC and PLA/CNC-g-PLLA melt-spun fibers collected using different speeds are shown in Figure 6. A continuous and homogeneous surface is observed for every fiber, as well as uniform diameters.

Moreover, SEM images do not reveal the presence of nanoparticles agglomerates along the fibers surface, which can be an evidence of well-dispersed cellulose nanocrystals in the PLA matrix. [40, 41] However, it can be seen from the SEM images that the increment on the collecting speed slightly increased the roughness along to the fibers. Cryo-fractured cross-sections of the fibers are shown in Figure 7. PLA reinforced with CNC and PLA reinforced with CNC-g-PLLA were homogenous and agglomerates of nanoparticles were not observed, which indicated well-dispersion of cellulose nanocrystals in the PLA matrix.

Thermal properties

It is well known that the processing conditions can strongly affected the final properties of the melt-spun fibers. So, in order to determine the effect of time and of temperature on the thermal degradation of the material during the melt-spinning process, thermal stability of raw PLA, PLA reinforced with CNC and PLA reinforced with CNC-g-PLLA before to feed the machine as well as their as-spun fibers have been analysed by TGA.

Figure 8A shows the results of the weight loss and Figure 8B the derivative of weight loss. As-spun fibers present thermal stability up to 300 °C.

In addition, in the case of raw PLA and PLA reinforced with cellulose nanocrystals grafted with PLA, the as-spun fibers show higher thermal stability than the feed materials. Moreover, the addition of nanocrystals increase the thermal stability of the nanocomposites, because of the higher thermal stability of the nanoparticles compared to the PLA.

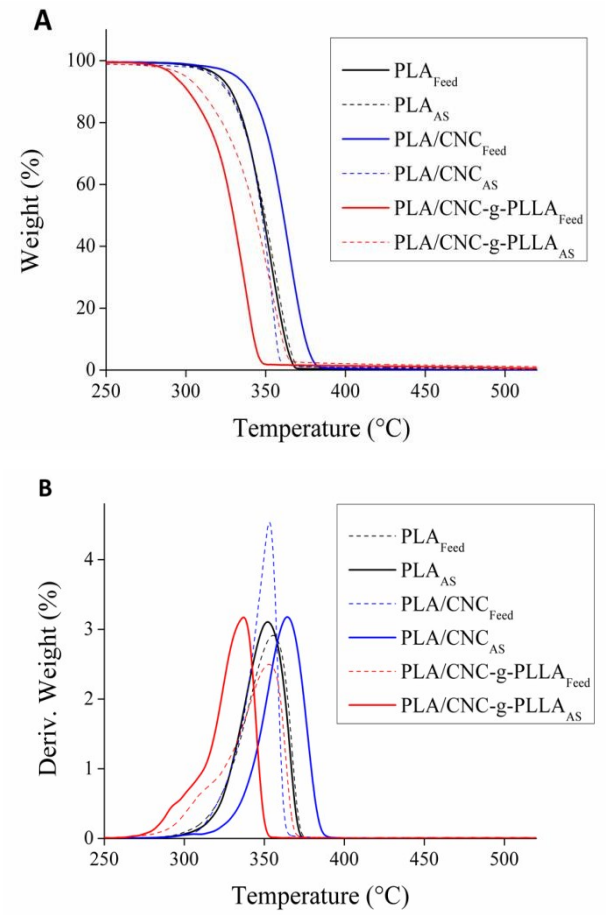

Fig. 8. Thermogravimetric analysis of the feed materials and as-spun fibers: A) weight loss profiles; B) normalized derivative of weight loss.

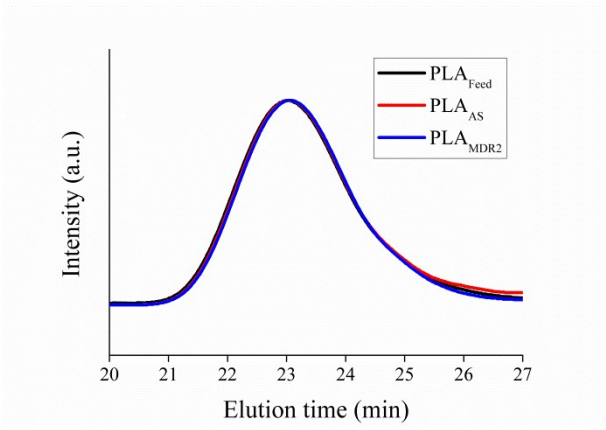

Fig. 9. GPC of the feed PLA, PLA fiber after spinning (PLA_{AS}) and PLA fiber after spun with highest speed (PLA_{MDR2}).

Molecular weight characterization was carried out by GPC in order to study the influence of temperature reached in the compounder into possible changes on the polymer molecular weight, as a consequence of chain-scissions. The PLA molecular weight has been evaluated comparing feed material (PLA_{Feed}) with as-spun fiber (PLA_{AS}) and fiber collected using the highest collected speed (PLA_{MDR2}), Figure 9. Both the molecular weight and the distribution of molecular weight keep on constant after melt-spinning process, so it is possible to conclude that the temperature used in the compounder does not affect the thermal stability of the materials.

Furthermore, the crystallinity of the melt-spun fibers can be strongly influenced by the processing conditions, such as melt-draw ratio. At this regards, WAXD and thermal analysis has been performed.

WAXD measurements are reported in Figure10A for PLLA, CNC and CNC-g-PLLA. Functionalized CNC show the diffraction peaks corresponding to both the PLLA and CNC. Moreover, WAXD measurements are reported in Figure10B for PLA_{MDR1}, PLA/CNC_{MDR1} and $PLA/CNC\text{-}g\text{-}PLLA_{MDR1}$ melt-spun fibers. The peak intensity corresponding to PLA crystals (Figure 10B) became stronger when nanoparticles were added, confirming that the crystallization process was favoured in the nanocomposite fibers.

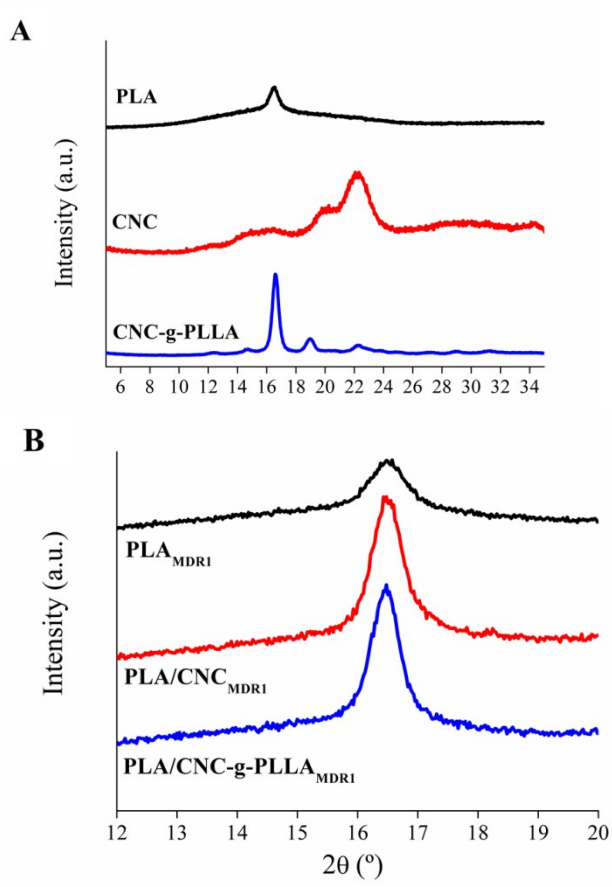

Fig. 10. WAXD measurements of A) PLA, CNC and CNC-g-PLLA and B) PLA_{MDR1}, PLA/CNC_{MDR1} and $PLA/CNC\text{-}g\text{-}PLLA_{MDR1}$ melt-spun fibers.

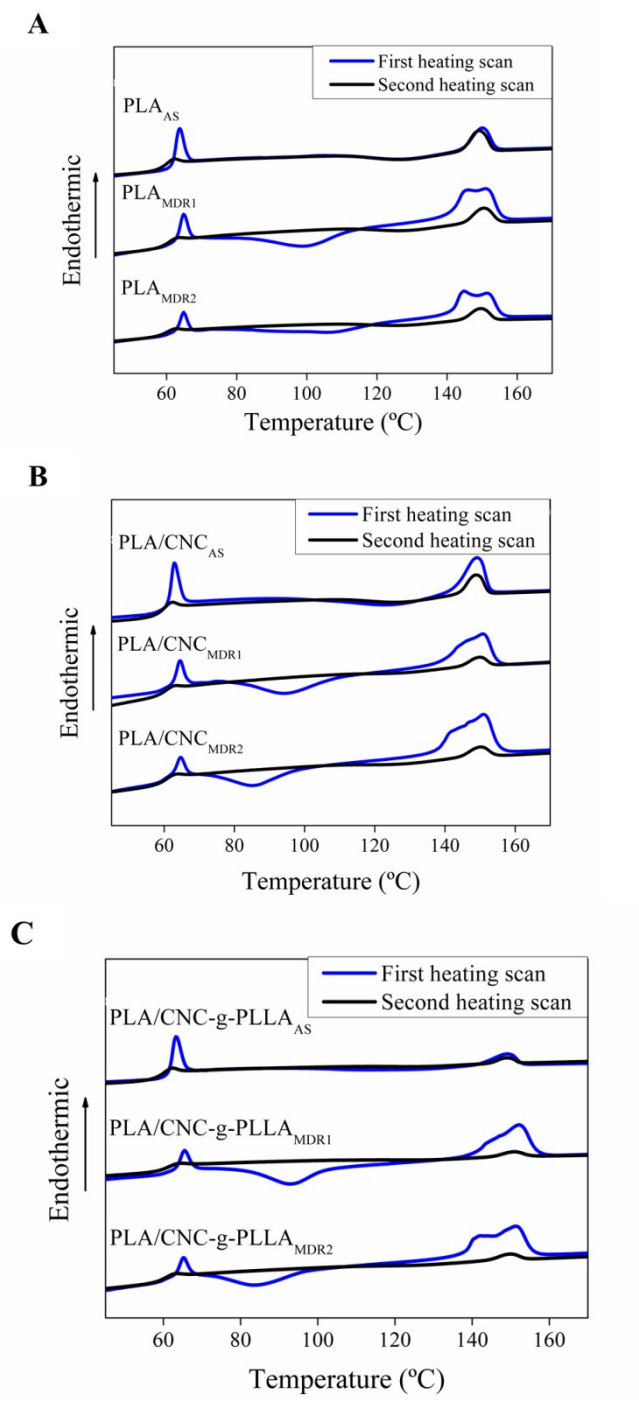

Fig. 11. Comparative DSC first and second heating scan curves of feed material and spun fibers collected using different speed of A) PLA, B) PLA/CNC and C) PLA/CNC-g-PLLA.

Figure 11 shows DSC thermograms corresponding to the first and second heating scan of melt-spun fibers of raw PLA (Fig. 11A), PLA reinforced with CNC (Fig. 11B) and PLA reinforced with CNC-g-PLLA (Fig. 11C) comparing fibers collected using different speed.

The experimental results are reported in Table 2. The degree of crystallinity determined from the first heating scan increases with increasing melt-draw ratio, as a consequence of molecular orientation also increases by increasing MDR. On the other hand, the degree of crystallinity increases with the addition of CNC-g-PLLA when the higher collector speed is used, so the influence of nanoparticles on the degree of crystallinity is more important when the melt-draw ratio is higher. This fact can be explain thus taking into account that cellulose nanocrystals are heterogeneous nucleation sites favouring of beginning of crystal growing.

In addition, nanocrystals produce a crystalline slide in the fibers surface called “transcrystalline slide”. [44] Moreover, in the case of nanocomposites, the cold crystallization temperature is lower than the one presented for the raw PLA.

Finally, the crystallization temperature decreases with increasing MDR. Even though the first heating scan is representative to study the thermal properties of fibers, as a consequence fiber structure disappear after this scan, in this case the second heating scan provides information about the chains orientation. Alignment of chains provides a residual high order, appearing crystallinity in the second heating.

Mechanical properties

Table 2. Main thermal characteristics obtained from first heating scan for melt-spun fibers collected using different speed of PLA, PLA/CNC and PLA/CNC-g-PLLA.

Materials	T_g (°C)	T_c (°C)	T_m (°C)	X_c (%)
PLA$_{AS}$	63	127	150	0.2
PLA$_{MDR1}$	64	100	151	8.8
PLA$_{MDR2}$	64	107	145	11.3
PLA/CNC$_{AS}$	62	123	149	5.8
PLA/CNC$_{MDR1}$	64	95	151	3.7
PLA/CNC$_{MDR2}$	64	85	151	14.4
PLA/CNC-g-PLLA$_{AS}$	62	124	149	1.3
PLA/CNC-g-PLLA$_{MDR1}$	64	93	152	7.1
PLA/CNC-g-PLLA$_{MDR2}$	64	84	151	15.0

The mechanical properties of melt spun fibers are summarized in Table 3. Generally, when comparing the fibers with different compositions and melt-draw ratios, the trend is that increased MDR as well as the addition of only 1 wt% CNC result in improved stiffness, strength and strain. These are remarkable results not seen before for spun PLA fibers. In an earlier study by John et al. [35] where CNC were used to reinforce melt spun PLA, the mechanical properties were not improved as seen in the present study. It is clearly seen that the main improvement here are caused by melt-drawing but if comparing the materials with the highest draw ratio, the modulus improved from 3455 MPa for neat PLA$_{MDR2}$ to 3852 MPa for PLA/CNC$_{MDR2\ and}$ to 4125 MPa for PLA/CNC-g-PLLA$_{MDR2.}$ At the same way the strength improved from 82 MPa for PLA$_{MDR2}$ to 118 MPa for PLA/CNC$_{MDR2}$ further to 171 MPa for the modified fibers PLA/CNC-g-PLLA$_{MDR2}$ and for the strain the improvement was from 5% > 51% > 91%. These great improvements are assumed to be due to the alignment of the CNC along to the fiber axis. A very large tensile strength improvement (234%) was observed for PLA/CNC-g-PLLA$_{MDR2}$ compared to PLA/CNC-g-PLLA$_{AS}$, which can be considered as an evidence of a flexible interface between CNC-g-PLLA and the PLA matrix and allowed this high stretching which is resulting to higher maximum strength.

Table 3. Tensile modulus max tensile strength and elongation at break of neat PLA and its melt-spun nanocomposite fibers, as spun and with different MDR.

Materials	Tensile Modulus (MPa)	Tensile Strength (MPa)	Elongation at break (%)
PLA_{AS}	1759 ± 119	53.5 ± 2.8	26.3 ± 12.5
PLA_{MDR1-A}	1652 ± 636	66.4 ± 2.3	47.7 ± 4.1
PLA_{MDR1}	2823 ± 130	77.8 ± 5.6	59.0 ± 7.8
PLA_{MDR2-A}	3091 ± 235	50.9 ± 4.2	4.9 ± 1.2
PLA_{MDR2}	3455 ± 158	82.2 ± 6.6	5.0 ± 1.1
PLA/CNC_{AS}	1918 ± 184	53.5 ± 0.9	21.3 ± 7.7
PLA/CNC_{MDR1-A}	1805 ± 369	58.8 ± 8.9	46.8 ± 4.4
PLA/CNC_{MDR1}	2943 ± 368	74.8 ± 7.7	60.9 ± 11.3
PLA/CNC_{MDR2-A}	3232 ± 764	51.6 ± 12.2	24.8 ± 4.2
PLA/CNC MDR2	3852 ± 241	118.5 ± 16.5	51.1 ± 11.3
$PLA/CNC\text{-}g\text{-}PLLA_{AS}$	2265 ± 366	51.2 ± 9.0	18.1 ± 6.9
$PLA/CNC\text{-}g\text{-}PLLA_{MDR1-A}$	2171 ± 101	47.2 ± 0.3	25.0 ± 11.5
$PLA/CNC\text{-}g\text{-}PLLA_{MDR1}$	2973 ± 214	65.8 ± 9.3	41.9 ± 3.2
$PLA/CNC\text{-}g\text{-}PLLA_{MDR2-A}$	3734 ± 382	74.0 ± 10.0	4.0 ± 0.5
$PLA/CNC\text{-}g\text{-}PLLA_{MDR2}$	4125 ± 440	171.0 ± 12.6	91.7 ± 12.2

Hooshmand et al. [41] discussed the effect of nanocellulose and molecular chain alignment on fiber mechanical properties in the study on melt-spun cellulose acetate butyrate nanocomposite fibers reinforced with CNC. The addition of CNC and CNC-g-PLLA had no significant effect on the tensile modulus and tensile strength of the as-spun fibers and fibers drawn at the lower draw ratio (MDR1) as indicate in Figure 12 which is reasonable result because the addition of CNC is only 1%. The reinforcing effect of the CNC and CNC-g-PLLA are more obvious when the nanocrystals are aligned to the direction of the fiber axis, especially in the higher draw ratio (MDR2). The fact that the tensile strength of the fibers reinforced with CNC and CNC-g-PLLA have been improved significantly, suggest the very good dispersion of the nanocrystals as well as a flexible interface between matrix and reinforcements.

Figure 12 summarizes the tensile modulus increases with the addition of both CNC and CNC-g-PLLA to the PLA matrix, as well as by increasing the draw ratio. The same trend was detected for the tensile strength (Fig. 12B) and for the elongation at break (Fig. 12C).

Conclusions

Nanocomposite melt spun fibers based on poly(lactic acid) and cellulose nanocrystals at 1 wt% (PLA/CNC) were prepared in two steps. First, neat PLA and nanocomposites microspheres obtained by using solvent evaporation method, starting from a DMF-PLA solution, based on thermally induced phase separation have been obtained. The prepared microspheres were spun to fibers using a micro twin-screw extrusion with a fiber drawing facility. Further, the CNC were successfully grafted with PLLA with the aim to improve the dispersion of the CNC and to create good interface between the CNC and PLA. FTIR and Raman spectroscopy, as well as TGA analysis and Molau test, confirmed the success of the grafting reaction. Presence of flow birefringence confirmed the good dispersion of CNC in the DMF-PLA solutions. It was also shown that melt-spun nanocomposites fibers did not degrade during the melt spinning process, since the GPC results did not show differences in the molecular weight or molecular weight distribution of spun fibers compared with the starting material.

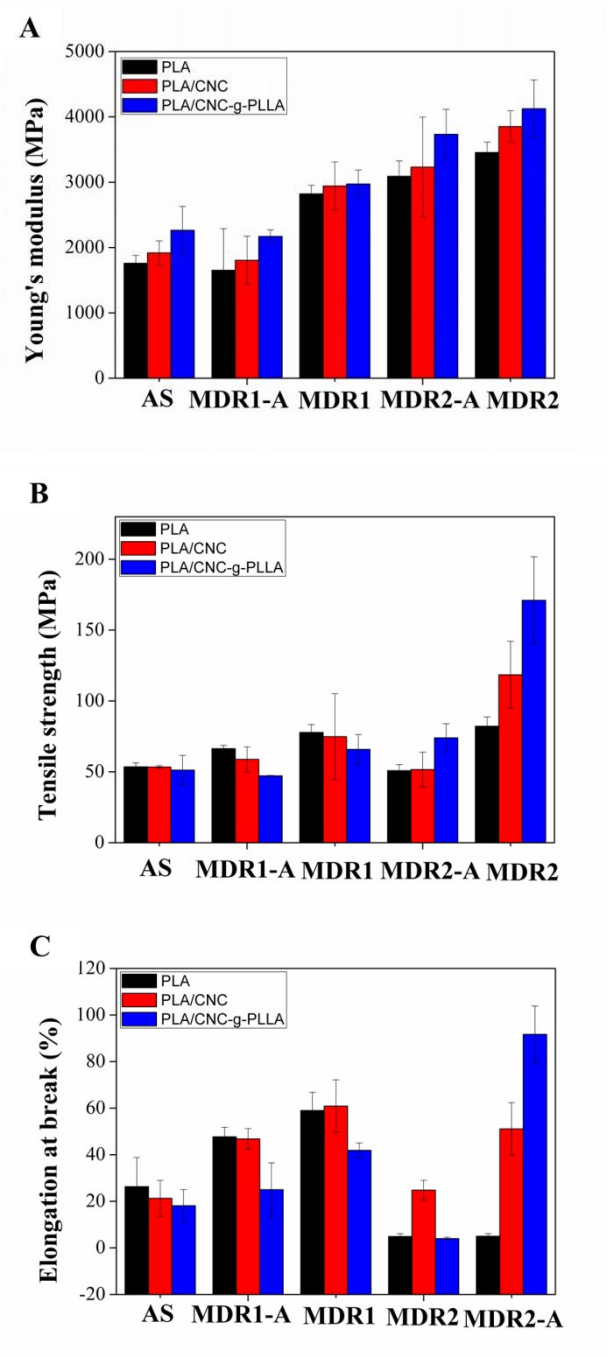

Fig. 12. The effect of 1 wt% CNC, modified CNC and draw ratios on: A) tensile modulus; B) strength and C) elongation at break.

The addition of cellulose nanocrystals was shown to increase the thermal stability of the nanocomposites, presenting higher influence into the degree of crystallinity than the melt-draw ratio. Finally, the mechanical properties of the PLA nanocomposite fibers were significantly improved with addition of only 1wt% CNC, with and without modification. The reinforcing mechanism is the alignment of the CNC and of PLA chains, we have earlier shown that such low amount of CNC alone cannot cause a such large increase but if the CNC together with the polymer is oriented, the orientation is very effectively reinforcing the fibers. However, the PLLA grafted nanocrystals (CNC-g-PLLA) resulted in increased strain and toughness. These results confirmed a better interfacial adhesion between CNC-g-PLLA and the PLA matrix indicating that grafting is positively affecting the properties acting as flexible interface between the nanocellulose and PLA leading to higher degree of alignment of the CNC and polymer molecular chains. Further, the dissolving process of PLA was successful to create good dispersion but need to be replaced with compounding extrusion to be able to produce these fibers at larger scale.

Acknowledgements

We are intended to the Spanish Ministry of Economy and Competitiveness (MAT2013-48059-C2-1-R and MAT2014-55778-REDT) and to the Regional Government of Madrid (S2013/MIT-2862) for their economic support. LP acknowledges also, the support of JAEDoc grant from CSIC cofinanced by FSE. The authors gratefully acknowledge the support of LLP/ERASMUS Placement (TUCEP) scholarship for research visit at Luleå University of Technology. Authors are also grateful for Bio4Energy, Swedish strategic research program for financial support.

Notes and references

‡ Footnotes relating to the main text should appear here. These might include comments relevant to but not central to the matter under discussion, limited experimental and spectral data, and crystallographic data.

§

§§

etc.

1 L. Peponi, D. Puglia, L. Torre, L. Valentini and J. M. Kenny, *Materials Science and Engineering: R: Reports*, 2014, **85**, 1-46.
2 V. J. Chen and P. X. Ma, *Biomaterials*, 2004, **25**, 2065-2073.
3 M. Persson, G. S. Lorite, S. W. Cho, J. Tuukkanen and M. Skrifvars, *ACS applied materials & interfaces*, 2013, **5**, 6864-6872.
4 M. Persson, S.-W. Cho and M. Skrifvars, *J Mater Sci*, 2013, **48**, 3055-3066.
5 A. L. Goffin, J. M. Raquez, E. Duquesne, G. Siqueira, Y. Habibi, A. Dufresne and P. Dubois, *Biomacromolecules*, 2011, **12**, 2456-2465.
6 L. Peponi, A. Mujica-Garcia and J. M. Kenny, Poly (lactic acid) Science and Technology: Processing, Properties, Additives and Applications, 171.
7 L. Fambri, A. Pegoretti, R. Fenner, S. D. Incardona and C. Migliaresi, *Polymer*, 1997, **38**, 79-85.
8 X. Yuan, A. F. T. Mak, K. W. Kwok, B. K. O. Yung and K. Yao, *Journal of Applied Polymer Science*, 2001, **81**, 251-260.
9 L. Peponi, I. Navarro-Baena, J. E. Báez, J. M. Kenny and A. Marcos-Fernández, *Polymer*, 2012, **53**, 4561-4568.
10 R. M. Rasal, A. V. Janorkar and D. E. Hirt, *Progress in Polymer Science*, 2010, **35**, 338-356.
11 R. Auras, B. Harte and S. Selke, *Macromolecular Bioscience*, 2004, **4**, 835-864.
12 P. Bordes, E. Pollet and L. Avérous, *Progress in Polymer Science*, 2009, **34**, 125-155.
13 M. Darder, P. Aranda and E. Ruiz-Hitzky, *Advanced Materials*, 2007, **19**, 1309-1319.
14 A. Sorrentino, G. Gorrasi and V. Vittoria, *Trends in Food Science & Technology*, 2007, **18**, 84-95.
15 Y. Habibi, L. A. Lucia and O. J. Rojas, *Chemical reviews*, 2010, **110**, 3479-3500.
16 D. Bondeson and K. Oksman, *Composites Part A: Applied Science and Manufacturing*, 2007, **38**, 2486-2492.
17 L. Petersson, I. Kvien and K. Oksman, *Composites Science and Technology*, 2007, **67**, 2535-2544.
18 D. Bondeson and K. Oksman, *Composite Interfaces*, 2007, **14**, 617-630.
19 K. Oksman, A. P. Mathew, D. Bondeson and I. Kvien, *Composites Science and Technology*, 2006, **66**, 2776-2784.
20 L. Petersson and K. Oksman, *Composites Science and Technology*, 2006, **66**, 2187-2196.
21 M. P. Arrieta, E. Fortunati, F. Dominici, E. Rayon, J. Lopez and J. M. Kenny, *Carbohydrate polymers*, 2014, **107**, 16-24.
22 A. Carlmark, E. Larsson and E. Malmström, *European Polymer Journal*, 2012, **48**, 1646-1659.
23 I. Navarro-Baena, J. M. Kenny and L. Peponi, *Cellulose*, 2014, **21**, 4231-4246.
24 M. S. Kim, J. C. Kim and Y. H. Kim, *Polymers for Advanced Technologies*, 2008, **19**, 748-755.
25 Y. Furuhashi, Y. Kimura and H. Yamane, *Journal of Polymer Science Part B: Polymer Physics*, 2007, **45**, 218-228.
26 Y. Nishimura, A. Takasu, Y. Inai and T. Hirabayashi, *Journal of Applied Polymer Science*, 2005, **97**, 2118-2124.
27 B. Gupta, N. Revagade, N. Anjum, B. Atthoff and J. Hilborn, *Journal of Applied Polymer Science*, 2006, **100**, 1239-1246.
28 B. Gupta, N. Revagade, N. Anjum, B. Atthoff and J. Hilborn, *Journal of Applied Polymer Science*, 2006, **101**, 3774-3780.
29 A. Mujica-Garcia, I. Navarro-Baena, J. M. Kenny and L. Peponi, *Journal of Renewable Materials*, 2014, **2**, 23-34.
30 F. Yang, R. Murugan, S. Wang and S. Ramakrishna, *Biomaterials*, 2005, **26**, 2603-2610.
31 A. Sonseca, L. Peponi, O. Sahuquillo, J. M. Kenny and E. Giménez, *Polymer Degradation and Stability*, 2012, **97**, 2052-2059.
32 V. Taubner and R. Shishoo, *Journal of Applied Polymer Science*, 2001, **79**, 2128-2135.
33 G. Schmack, B. Tändler, R. Vogel, R. Beyreuther, S. Jacobsen and H. G. Fritz, *Journal of Applied Polymer Science*, 1999, **73**, 2785-2797.
34 J. Cicero and J. Dorgan, *Journal of Polymers and the Environment*, 2001, **9**, 1-10.
35 M. J. John, R. Anandjiwala, K. Oksman and A. P. Mathew, *Journal of Applied Polymer Science*, 2013, **127**, 274-281.
36 J. J. Blaker, K.-Y. Lee, M. Walters, M. Drouet and A. Bismarck, *Reactive and Functional Polymers*, 2014, **85**, 185-192.
37 E. D. Cranston and D. G. Gray, *Biomacromolecules*, 2006, **7**, 2522-2530.
38 E. Fortunati, I. Armentano, Q. Zhou, A. Iannoni, E. Saino, L. Visai, L. A. Berglund and J. M. Kenny, *Carbohydrate Polymers*, 2012, **87**, 1596-1605.
39 M. A. S. Azizi Samir, F. Alloin, J.-Y. Sanchez, N. El Kissi and A. Dufresne, *Macromolecules*, 2004, **37**, 1386-1393.
40 S. Hooshmand, S.-W. Cho, M. Skrifvars, A. Mathew and K. Oksman, *Plastics, Rubber and Composites*, 2014, **43**, 15-24.

41 S. Hooshmand, Y. Aitomäki, M. Skrifvars, A. P. Mathew and K. Oksman, *Cellulose*, 2014, **21**, 2665-2678.
42 N. Naseri, C. Algan, V. Jacobs, M. John, K. Oksman and A. P. Mathew, *Carbohydrate Polymers*, 2014, **109**, 7-15.
43 N. Lin, G. Chen, J. Huang, A. Dufresne and P. R. Chang, *Journal of Applied Polymer Science*, 2009, **113**, 3417-3425.
44 D. Liu, X. Yuan and D. Bhattacharyya, *Journal of Materials Science*, 2011, **47**, 3159-3165.

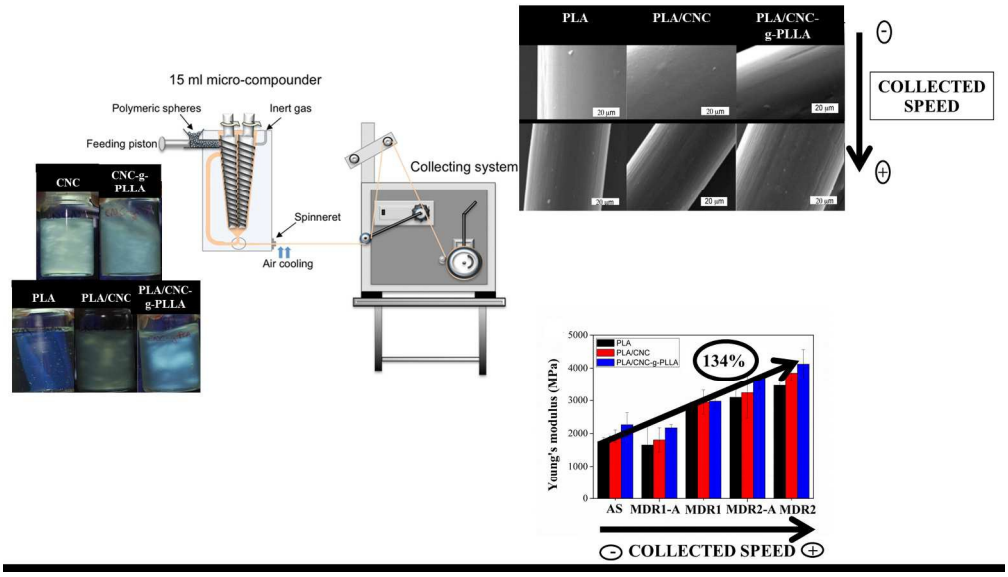

372x212mm (150 x 150 DPI)